CHEMICAL ENGINEERING TRANSACTIONS
VOL. 101, 2023
A publication of AIDIC
The Italian Association of Chemical Engineering
Online at www.cetjournal.it
Guest Editors: Paolo Ciambelli, Luca Di Palma

ISBN 979-12-81206-00-7; **ISSN** 2283-9216
DOI: 10.3303/CET23101025

Antifungal Properties of Silver Nanoparticles Produced by Green Synthesis with Extract of Red Seaweed *Chondracanthus chamissoi*

Rita J. Cabello-Torres[a]*, Deyanira K. Castillo[a], Carlos A. Castañeda-Olivera[a], Daniel F. Neciosup[a], Edison A. Romero-Cabello[b], Noemi R. Checca[c]

[a]Universidad César Vallejo, Campus San Juan de Lurigancho, Lima, Perú
[b]Universidad Nacional Agraria la Molina, La Molina, Lima Peru
[c]Brazilian Center for Physics Research, R. Dr. Xavier Sigaud 150, 22290-180, Rio de Janeiro-RJ, Brazil.
rcabello@ucv.edu.pe

The green synthesis of metal nanoparticles is an eco-friendly and promising approach for various applications including silver nanopesticides with seaweed extract. The aim of the research has been to synthesize silver nanoparticles (AgNPs), using extract of red seaweed *Chondracanthus chamissoi* and evaluate their antifungal properties. The methodology consisted in the aqueous extraction of the seaweed and combination with an $AgNO_3$ solution in hot. The crystallinity, morphology and chemical composition were studied by XRD, SEM and EDS. Antifungal tests were carried out againt the fungus *Fusarium Solani*, three doses of AgNPs (10 %, 20 % and 30 %) were applied under laboratory conditions. The diffractogram revealed AgCl as the main phase and Ag as the secondary phase. The SEM showed cubes de AgCl with a size of ~350 nm and Ag spherical nanoparticles (NPs) with a size of ~55 nm, while AgNPs decorated the AgCl cubes. This AgCl size could be related to partial reductions or unreacted ions. The antifungal activity showed a greater efficacy of AgNPs the increase in the AgNPs dose decreased the growth of *F. solani*, the 30 % AgNPs dose did not record the diameter of the fungus. It is concluded that the AgNPs produced by green synthesis using the red seaweed *Chondracanthus chamissoi* turns out to be an effective process for its application as an antifungal product.

1. Introduction

Nanoparticles (NPs) are produced by physical, chemical and biological methods with certain particular advantages and disadvantages according to their final applications (Real and Benites, 2021). Silver nanoparticles (AgNPs) have a variety of applications in different fields due to their superior physicochemical and biological properties (Rozhin et al., 2021). Hassan et al. (2021) showed that Ag/AgCl NPs are excellent pathogen agents and inhibitors. *Chondracanthus chamissoi* (Kützing, 1843), is a red seaweed (Phylum: Rhodophyta; Subphylum: Eurhodophytina; Class: Florideophyceae; Subclass: Rhodymeniophycidae; Order: Gigartinales; Family: Gigartinaceae; Genus: Chondracanthus), it has a ramified form that reaches 60 cm long, it has abundant cystocarps which generate the spores, they are generally fixed on intertidal and subtidal rocks, by means of their fixing disk and inhabits Peru from the coasts of Paita (Piura) and the Libertad Region extending to the south of the country (Rodríguez et al. 2018). This species has a wide domestic use in coastal meals (Cabello-Torres et al., 2022) and commercial interest (Rodríguez et al., 2018). *C. chamissoi* is an abundant macroalgae in Peru, it is a species of Rhodophyta known as "Yuyo", "mococho" of great commercial importance, due to its carrageenan content; with a growing demand in the market (2.50 dollars/kg) (Arbaiza et al., 2019). It contains amino acids such as leucine, valine, phenylalanine, lysine, serine, glycine, glutamic acid among others (Vilcanqui et al., 2021). Ghareb et al. (2020) reported recent applications of macroalgae in the green synthesis of metallic nanoparticles, by sulfated polysaccharides organized as carrageenan in red algae (AlNadhari et al., 2021). Water is generally used to dissolve polyphenols and proteins that are reducing and stabilizing agents that inhibit particle agglomerations during chemical synthesis (Mondal et al., 2020).

Paper Received: 17 January 2023; Revised: 20 March 2023; Accepted: 28 May 2023
Please cite this article as: Cabello Torres R.J., Castillo D.K., Castaneda-Olivera C.A., Neciosup D.F., Romero-Cabello E.A., Checca N.R., 2023, Antifungal Properties of Silver Nanoparticles Produced by Green Synthesis with Extract of Red Seaweed Chondracanthus Chamissoi, Chemical Engineering Transactions, 101, 145-150 DOI:10.3303/CET23101025

There is very little background on the application of seaweed in the green synthesis of nanoparticles, and specifically on red seaweed such as *C. chamissoi* in the synthesis of AgNPs. The size, shape, and other properties of the nanoparticles depend on the operating conditions and the macroalgae biomolecules that react during reduction/stabilization (Roselini et al., 2019). The initial color change to brown tones on synthesis is due to metallic reduction of Ag^{+} to Ag^{0} (Anjali et al., 2022).
This research offers a new approach on the synthesis of AgNPs (Ag^{0} and AgCl-NP), taking into account that the genus *Chondracanthus* is distributed in more than thirteen countries on different coasts and in four oceans of both hemispheres (Bulboa et al., 2020). The objective of the research was the green synthesis of AgNPs using the aqueous extract of the red seaweed *C. chamissoi* as Ag ion reducing agent and AgNPs stabilizing agent; from a very simple one-step method and its application as an antifungal agent, against the potato fungus *Fusarium Solani*; which also attacks a variety of plants, in this case it infects the potato and ends with a dry rot, a serious disease that affects the various potato tubers (Pour et al., 2019).

2. Materials and methods

2.1 Obtaining red seaweeds and extraction

Around 1,000 g of *Chondracanthus chamissoi* were collected on the Malabrigo beach in the La Libertad Region (Peru), during the summer of 2022. The sample was immediately washed with seawater to remove foreign material and after with tap water. The seaweed was then spread on blotting paper placed in the shade exposed to dryness at room temperature. Once dry, the sample was ground in a mortar until a fine powder was obtained. Then, 5 g of the dry red seaweed powder were weighed and added to 100 mL of distilled water in a 250 mL beaker, which was heated at 60 ºC for 30 min. The suspension was filtered with Whatman Nº 1 filter paper, the aqueous extract was separated and stored at 4 ºC for its correct use.

2.2 Green Synthesis of Ag Nanoparticles (AgNPs)

A solution of $AgNO_3$ (1mM) was prepared and then 95 mL was combined with 5 mL of the aqueous extract of *C. chamissoi*. The mixture was stirred for 30 min at 100 ºC and then at 90 ºC for 1.5 h. A color change from pale yellow to dark brown indicated the formation of AgNPs. The generated suspension was centrifuged at 5,000 rpm for 20 min (Boeco Centrifuge SC-8; Germany) and then the liquid was separated, while the sediments made up of the AgNPs were collected and dried at room temperature for characterization. The same process was applied to the control sample made up only of the algae extract, which did not change color and served as an indicator in contrast to the formation of the AgNPs (Gauri et al., 2016) (See Figures 1a-1f).

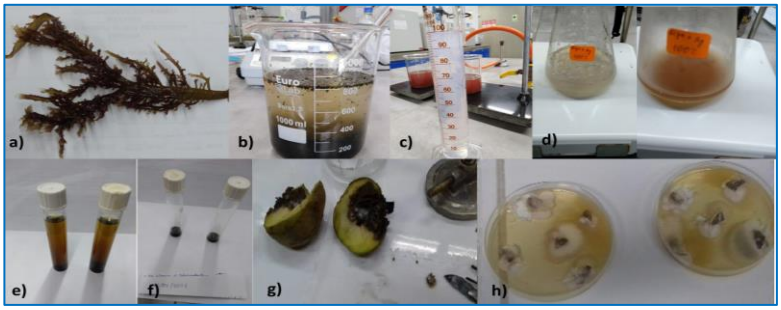

Figure 1. Green synthesis: a) C. chamissoi seaweed; b) aqueous extract of seaweed; c) $AgNO_3$ (1 mM); d) AgNPs formation, color change (brown); e) suspension; f) AgNPs; g) infected potato and h) F. solani isolated

2.3 Characterization of AgNPs

Ag/AgCl nanoparticles formation were confirmed by UV-visible spectrophotometry (200 to 700 nm) (GENESYS™ 10S spectrometer, U.S.). Metallic silver presents an optical absorption in this range, explained by the resonance of surface plasmons (González-Ballesteros et al., 2020); it is a consequence of the reduction (Ag^{0}) and stabilization (Ag^{0}, Ag^{+}) produced by the aqueous extract of *C. chamissoi*. Morphological characterization was performed by scanning electron microscopy (SEM) using the high resolution 15 kV TESCAN LYRA-3 equipment coupled with the EDS detector (OXFORD INSTRUMENTS, United Kingdom). Energy dispersive X-ray spectroscopy (EDS) was applied to establish the elemental composition of the Ag/AgC-NPs. Crystallographic analysis was performed by comparing the XRD and SEM results with crystallographic sheets from the Inorganic Crystal Structures Database (ICSD: code #22434 and code #56538, for Ag^{0} and AgCl).

2.4 Isolation of the *Fusarium solani* from potato

The method of Kalman et al. (2020), with certain modifications, to isolate *F. Solani* from potato, the affected part was separated, disinfected and cultured on potato dextrose agar (PDA); for 7 d at 30 °C. (See Figures 1g and 1h). For this purpose, the *Fusarium Solani* fungus was isolated from pieces of infected potato skin (1x1 cm), for which the sample was soaked for 1 minute in a sodium hypochlorite solution (2 %), rinsed with millipore water and dried on tissue paper. Then inoculated on acidified potato dextrose agar (PDA) 25 % with lactic acid placed in a Petri dish and incubated for 7 d at 26 °C. Subsequently, the *F. solani* mycelia were repeatedly isolated for purification in PDA medium and incubated for 7 d at 26 °C. As a result of the purification, the culture was treated with AgNPs.

2.5 Antifungal Activity

The Petri disk-dish antibiogram assay was performed by adding 10 ml of 3% potato dextrose agar (PDA) on the glass plate. The PDA was prepared following the method applied by Roseline et al. (2019), and on that layer the *F. solani* fungal mycelia mixed preliminarily with PDA (1.5 %) were added. A Whatman Nº 1 paper discs of 6 mm in diameter were impregnated with the AgNPs in doses of 10, 20 and 30 % (w/v), each one was deposited aseptically on the plates. Finally, all the plates were incubated at 35 ºC for 3, 5, and 7 d. Each test had 5 replicates. The inhibitory effect was calculated as the percentage of the inhibition rate (Rentería et al., 2019):

$$IR\% = (\frac{(D_1 - D_2}{D_1})(100\%) \quad (1)$$

Where, D_1 is the diameter of the control fungal mycelium and D_2 the diameter of the mycelium grown in the presence of AgNPs.

2.6 Analysis of data

A descriptive and inferential analysis of the resulting data was applied using the Excel program, the surface response method (RSM) was also applied to analyze the effect of both factors (dose and days of treatment) on the growth and inhibition of the fungus. Both response variables were modeled based on the factors of interest, for which the Minitab 19 statistical software was used. The reliability of the results was determined using the p-value and the correlation coefficient R^2 used as decision parameters in the statistical analysis.

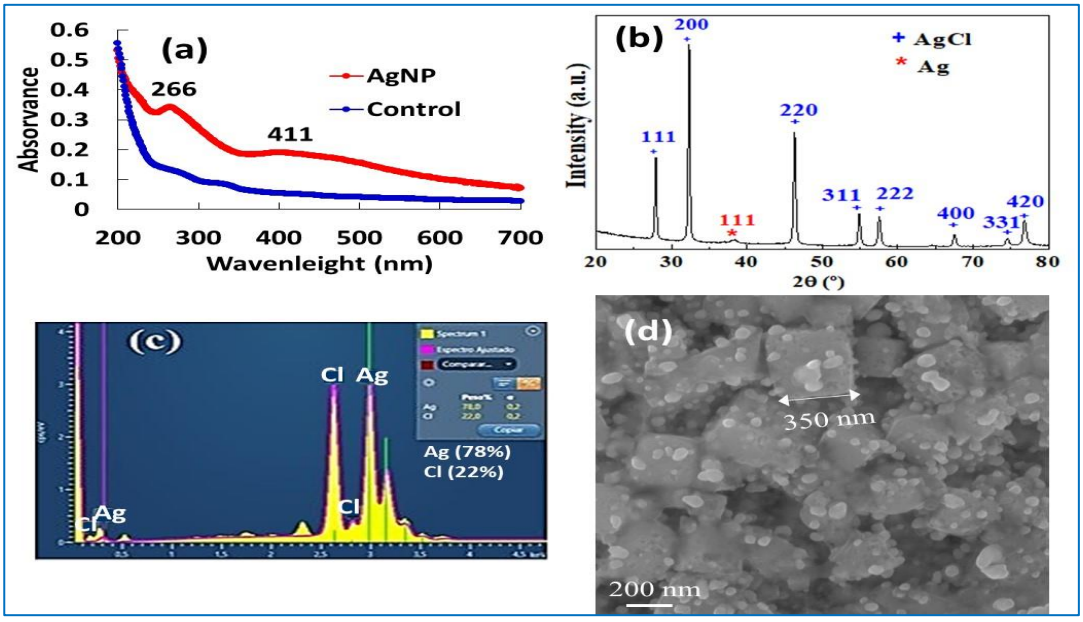

Figure 2: Characterization of AgNPs: a) UV-Visible spectrum for AgNPs and control; b) XRD spectra of AgNPs; c) EDX spectrum (AgNPs composition); d) SEM micrograph of AgNPs.

3. Results and Discussion

3.1 Observation of the formation of nanoparticles by UV-Visible spectrum

After adding the seaweed extract to the $AgNO_3$ solution, the green synthesis process initially showed a turbid yellowish coloration and after one hour a brown color indicating the formation of AgNPs in the oxidation-

reduction reaction; the "control" solution did not present any color change. Using the UV-visible spectrum, the formation of AgNPs was confirmed from absorption peaks generated between 395 and 411 nm, very close (410 nm) to that produced by Roseline et al. (2019) and 266 nm can be attributed to AgCl NPs (Hassan et al., 2021). This color change to brown is a characteristic of AgNPs excitation of monodisperse spherical shape (Princy and Gopinath, 2021); caused by surface plasmon resonance (SPR) (Jebril et al., 2020), not observed for the "control" solution (Figure 2a).

3.2 Morphological and chemical characteristics of AgNPs

The Figure 2b shows diffraction peaks (XRD) similar to those reported by Dong et al. (2021), with planes (111), (200), (311) and (222) attributed mainly to the formation of AgCl crystals of cubic shape and the plane (111) assigned to Ag^0, this means that the Ag^+ ions reacted with the chloride present coming from the nature of the red seaweed, another group of Ag^+ was reduced to Ag crystals. The organic peaks of the algae were not observed, probably due to the overlap of the Ag/AgCl crystalline peaks. Energy dispersive X-ray (EDX) spectrometry (Figure 2c) showed elemental silver and AgCl atoms in the NPs structure; conformed mainly by atoms of Ag (78 %; σ=0.2), Cl (22 %; σ=0.2). This occurred because metallic silver presents an optical absorption in this range, explained by surface plasmon resonance (Kurt and Çelik, 2020, Hassaan and Hosny, 2018); as a consequence of the reduction produced by the extract *C. chamissoi* from Ag^+ ions to Ag^o**.** The SEM image (Figure 2d) shows the synthesized AgNPs with spherical shapes, with sizes smaller than 55 nm and well distributed without aggregation on the AgCl (-350 nm). This size of diameter could be related to the partially reduced Ag ions or unreacted ions (Hassan et al., 2021).

3.3 Growth of F. solani with and without treatment (AgNPs)

Figure 3 shows the growth of the *F. solani* colony (control) measured on day 1, 3, 5 and 7 with 5 replicates per day. Once the AgNPs were synthesized, 3 doses (10, 20 % and 30 %, w/v) were applied to the colonies of the fungus on day 1. The fungal growth was measured by diameters to analyse the antifungal activity. It was evidenced that the control samples increased from 33.7 to 89.9 mm in diameter over the days; while the increase in the AgNPs dose decreased the growth of *F. solani*, the 30 % AgNPs dose did not record the diameter of the fungus.

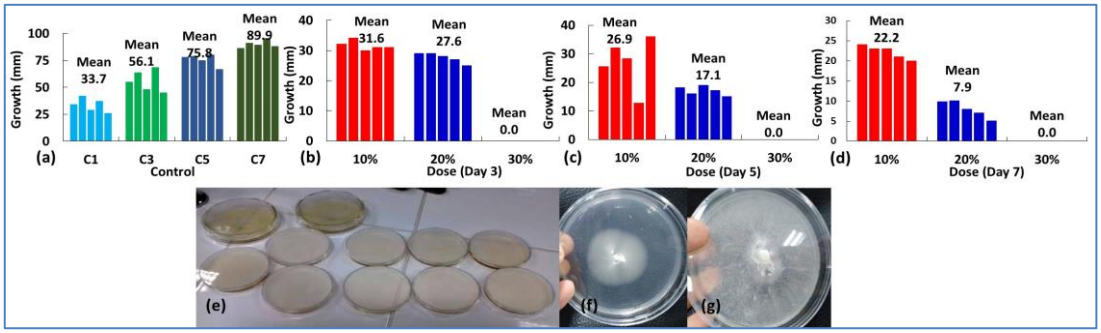

Figure 3: F. solani: a) growth of control samples per day; b) treatment- 3 d; c) treatment-5 d; d) treatment-7 d; e) treatment replicates, f) 30% AgNP inhibition, g) control without AgNPs

3.4 Dose-day Antifungal effect of AgNPs against *Fusarium solani*

Table 1 shows the Analysis of Variance (ANOVA) using the Response Surface method (RSM) to analyze the effect of AgNPs Doses and days of treatment on the growth, and inhibition rate of *F. solani*.

The response surface design (RSM) was applied to better understand the "Dose" and "Days" factors manipulated with the application of AgNPs and optimize the experimental response focused on: a) growth and b) inhibition of the fungus in the treatments developed (Table 1). This methodology provided a statistically significant quadratic term addition model ($p < 0.05$) for both fungal responses, demonstrating the association between growth (and inhibition) and each model term Figure 4a shows that when a higher dose of $AgNO_3$ is applied, despite the passage of days, the growth of the fungus is not significant, so there is no difference between the treatment of one day or 7 d. On the other hand, the factor "dose" was significant ($p < 0.05$) for the growth of the fungal mycelium in the quadratic model, also observed in the value of F (F_{Dose}=293.1 > D_{Day}=0.98) from Table 1. Regarding the "inhibition" of the fungus (Figure 4b), both variables were significant ($p<0.05$), this was demonstrated by the best fit achieved (R^2 = 0.87). The model also explains the interaction "dose*day" on the rate of inhibition (significant; p = 0). Therefore, a maximum dose of 30 % of AgNPs did not allow the growth of the fungus from the third day, inhibiting it 100 %, and germination was possibly inhibited due to the formation of pores in the cell walls that led to cell death (Ghojavand et al., 2020; Jalal et al., 2018; Pal et al., 2021).

Table 1: ANOVA: Response Surface Regression: Growth and % Inhibition rate versus Dose (%); Day

Description	DF	Sum of Squares	Mean Square	F Value	P Value	DF	Sum of Squares	Mean Square	F Value	P Value
Growth (mm)						Inhibition rate (%)				
Model	5	43,193.5	8,638.7	84.3	0	5	123,020	24,603.9	107.98	0
Linear	2	30,136.8	15,068.4	147.04	0	2	99,833	49,916.5	219.07	0
Dose	1	30,036	30,036	293.1	0	1	54,856	54,855.9	240.75	0
Day	1	100.8	100.8	0.98	0.325	1	44,977	44,977.2	197.39	0
Square	2	2,559.1	1,279.6	12.49	0	2	11,814	5,907.1	25.92	0
Dose*Dose	1	2,435.6	2,435.6	23.77	0	1	3,103	3,103.1	13.62	0
Day*Day	1	123.5	123.5	1.2	0.276	1	8,711	8,711.1	38.23	0
2-Way Interaction	1	10,497.6	10,497.6	102.44	0	1	11,372	11,372.3	49.91	0
Dose*Day	1	10,497.6	10,497.6	102.44	0	1	11,372	11,372.3	49.91	0
Error	74	7,583.3	102.5			74	16,861	227.9		
Lack-of-Fit	10	6,000.7	600.1	24.27	0	10	15,488	1,548.8	72.17	0
Pure Error	64	1,582.6	24.7			64	1,373	21.5		
Total	79	50776.8				79	139,881			

The growth prediction and inhibition rate are shown in Figure 4.

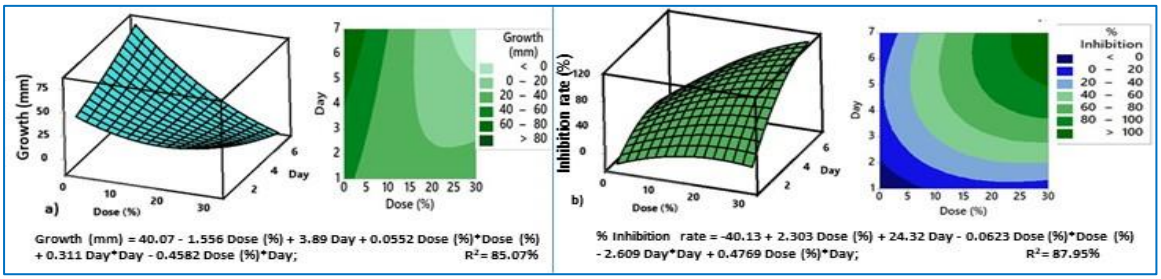

Figure 4: Dose-Day response surface plot: a) Fusarium Solani growth and b) % inhibition of Fusarium Solani growth

4. Conclusion

Silver nanoparticles (Ag^0 and AgCl) have been synthesized by applying extract of the *Chondracanthus chamissoi* (red seaweed). The AgNPs presented spherical shapes with sizes smaller than 50 nm distributed without agglomeration on saline cells. AgNPs showed successful antifungal activities against *F. solani*. The response surface method (RSM) generated significant ($p< 0.05$) and robust ($R^2 > 0.8$) quadratic models. It was shown that the factors "Dose" and "Days" affected the inhibition of the fungus and that only the factor "Dose" was enough to affect the growth of the fungus. The application of 30 % $AgNO_3$ in the mycelia culture did not allow the growth of the fungus from the third day of treatment. These results show that the green synthesis of AgNPs-seaweed extract has antifungal properties and also opens up new avenues of research in the applications of these nanoparticles.

Acknowledgments

The authors would like to thank CAPES, CNPQ and FAPERJ for grants and LABNANO/CBPF for technical support during the electron microscopy work; and "Investiga UCV" of the Universidad César Vallejo for financial support for the publication of this research.

References

AlNadhari S., Al-Enazi N. M., Alshehrei F., Ameen F., 2021, A review on biogenic synthesis of metal nanoparticles using marine algae and its applications, Environmental Research, 194, 110672.

Anjali R., Palanisamy S., Vinosha M., Selvi A. M., Sathiyaraj G., Marudhupandi T., Mohandoss S., Prabhu N.M., You S., 2022, Fabrication of silver nanoparticles from marine macro algae Caulerpa sertularioides: characterization, antioxidant and antimicrobial activity, Process Biochemistry, 121, 601-618

Arbaiza S., Gil-Kodaka P., Arakaki N., Alveal K., 2019, Primeros estadios de cultivo a partir de carpósporas de Chondracanthus chamissoi de tres localidades de la costa peruana, Revista de biología marina y oceanografía, 54(2), 204-213

Bulboa C.C., Massad I.P., Contreras-Porcia L., Zapata J., Castañeda F., Ramírez M.E., Gil-Kodaka P., 2020, Concise review of genus Chondracanthus (Rhodophyta: Gigartinales), Journal of applied phycology, 32(2), 773-785.

Cabello-Torres R.J., del Pino L.F., Alegría-Arnedo M.C., Rodriguez-Rodriguez M., Valdiviezo-Gonzales L., 2022, Decontamination kinetics of tannery waters using bioflocculants, Tecnología y Ciencias del Agua, 13(6), 1-53

Dong Y.Y., Zhu Y.H., Ma M.G., Liu Q., He, W.Q., 2021, Synthesis and characterization of Ag@ AgCl-reinforced cellulose composites with enhanced antibacterial and photocatalytic degradation properties, Scientific Reports, 11(1), 1-9.

Gauri B., Vidya K., Sharada D., Shobha W., 2016, Synthesis and characterization of Ag/AgO nanoparticles as alcohol sensor, Res J Chem Environ, 20(10), 1-5

Ghojavand S., Madani M., Karimi J., 2020, Green synthesis, characterization and antifungal activity of silver nanoparticles using stems and flowers of felty germander, Journal of Inorganic and Organometallic Polymers and Materials, 30(8), 2987-2997.

González-Ballesteros N., Rodríguez-Argüelles M. C., Lastra-Valdor M., González-Mediero G., Rey-Cao S., Grimaldi M., Cabaza A., Bigi F., 2020, Synthesis of silver and gold nanoparticles by Sargassum muticum biomolecules and evaluation of their antioxidant activity and antibacterial properties, Journal of Nanostructure in Chemistry, 10(4), 317-330.

Hassaan M. A., Hosny S., 2018. Green synthesis of Ag and Au nanoparticles from micro and macro algae-review, International Journal of Atmospheric and Oceanic Sciences, 2(1), 10-22.

Hassan K.T., Ibraheem I.J., Hassan O.M., Obaid A.S., Ali H.H., Salih T.A., Kadhim M.S., 2021, Facile green synthesis of Ag/AgCl nanoparticles derived from Chara algae extract and evaluating their antibacterial activity and synergistic effect with antibiotics, Journal of Environmental Chemical Engineering, 9(4), 105359.

Jebril S., Jenana R.K.B., Dridi C., 2020, Green synthesis of silver nanoparticles using Melia azedarach leaf extract and their antifungal activities: In vitro and in vivo, Materials Chemistry and Physics, 248, 122898.

Kalman B., Abraham D., Graph S., Perl-Treves R., Meller H.Y., Degani O., 2020, Isolation and identification of Fusarium spp., the causal agents of onion (Allium cepa) basal rot in Northeastern Israel, Biology, 9(4), 69.

Kurt A., Çelik Y., 2020, Synthesis of quasi-spherical silver nanoparticles by chemical reduction route using different reducing agents, Konya Journal of Engineering Sciences, 8 (4), 828-838

Kützing FT., 1843, Phycologia Generalis oder Anatomie, Physiologie und Systemkunde der Tange, Leipzig, Deutschland, Brockhaus, 458.

Mondal P., Anweshan A., Purkait M. K., 2020, Green synthesis and environmental application of iron-based nanomaterials and nanocomposite: a review, Chemosphere, 259, 127509.

Pal A., Goswami R., Roy D.N., 2021, A critical assessment on biochemical and molecular mechanisms of toxicity developed by emerging nanomaterials on important microbes, Environmental Nanotechnology, Monitoring & Management, 16, 100485.

Pour M.M., Saberi-Riseh R., Mohammadinejad R., Hosseini A., 2019, Investigating the formulation of alginate-gelatin encapsulated Pseudomonas fluorescens (VUPF5 and T17-4 strains) for controlling Fusarium solani on potato, International journal of biological macromolecules, 133, 603-613.

Princy K. F., Gopinath A., 2021, Green synthesis of silver nanoparticles using polar seaweed Fucus gardeneri and its catalytic efficacy in the reduction of nitrophenol, Polar Science, 30, 100692.

Real C., Benites E., 2021, Green Silver Nanoparticles for Effluent Treatment with Brl Blue Dye in the Textile Industry, Chemical Engineering Transactions, 84, 223-228.

Rentería M.E., Ochoa M. A., Guzmán O.J.M., Barrera S.M.Á., Fernández H. E., Moreno S.S.F., 2019, Actividad in vitro de promoción del crecimiento vegetal y control biológico de rizobacterias aisladas de zacate bermuda ruderal, Revista mexicana de ciencias agrícolas, 10(2), 311-324

Rodríguez E.F., Fernández H.M.A., Alvítez I.E., Pollack V.L.E., Luján B.L.A., Geldres C.C.W., Paredes P.Y., 2018, Algas marinas del litoral de la región La Libertad, Perú, Scientia Agropecuaria, 9(1), 71-81.

Rozhin A., Batasheva S., Kruychkova M., Cherednichenko Y., Rozhina E., Fakhrullin R., 2021, Biogenic silver nanoparticles: Synthesis and application as antibacterial and antifungal agents, Micromachines, 12(12), 1480.

Vilcanqui Y., Mamani-Apaza L.O., Flores M., Ortiz-Viedma J., Romero N., Mariotti-Celis M.S., Huamán-Castilla N.L., 2021, Chemical Characterization of Brown and Red Seaweed from Southern Peru, a Sustainable Source of Bioactive and Nutraceutical Compounds. Agronomy, 11(8):1669.